

Perception Enhancement for Autonomous Vehicles in Foggy Conditions

Shimaa Ragab, Moustafa Elgendy, and Ahmed Shalaby¹.

¹ Department of Computer Science, Faculty of Computers and Artificial Intelligence, Benha University, Banha, 13511, Egypt

ABSTRACT Autonomous vehicles face significant challenges in adverse weather conditions, such as fog, which reduces visibility and degrades the quality of camera-captured images, making it difficult to detect targets and obstacles. Developing an effective image-defogging algorithm is crucial to enhancing the optical system's ability to adapt to varying environmental conditions. In this work, we apply a denoising autoencoder-based approach to address the fog removal problem, as it has demonstrated fast and efficient results. Unlike traditional methods that train the model on the original data, this approach trains the model on the noise present in the input data, as noise is simpler to regenerate than the original data. Noise reduction is then performed by subtracting the extracted noise from the noisy input. To further enhance the model's performance, we focus on improving the feature extraction process by incorporating architectural optimizations, such as the use of skip connections and advanced data augmentation techniques. Various optimizers are also compared to achieve better accuracy. The model's performance is evaluated using SSIM and PSNR metrics, with results showing PSNR and SSIM values of 26.03 and 0.939, respectively, for the outdoor dataset, and 29.87 and 0.966 for the indoor dataset when applied to the RESIDE dataset.

INDEX TERMS Autonomous vehicles, Adverse weather conditions, Perception and sensing, Deep learning.

I. INTRODUCTION

Autonomous vehicles (AVs) are revolutionizing transportation through the integration of artificial intelligence (AI), advanced sensors, and real-time decision-making systems. These vehicles offer the potential for safer, more efficient, and accessible mobility by minimizing human error, reducing traffic congestion, and providing transportation solutions for individuals with mobility limitations[1].

Despite significant advancements, autonomous vehicles face critical challenges in adverse weather conditions, particularly fog. Fog reduces visibility, degrades image contrast, and severely impacts the performance of visual sensors, making object detection and scene understanding more difficult [2], [3]. Such conditions can impair the reliability of autonomous driving systems (ADS), raising safety concerns.

Although there have been significant advancements, adverse weather conditions, especially fog, present serious challenges to autonomous driving systems (ADS). Fog can significantly degrade sensor performance and reduce the ability to accurately detect and classify objects, leading to impaired decision-making capabilities [4],[5],[6],[7],[8].

Poor visibility in fog results in low-contrast images, making it difficult to capture fine structural details[9].

To mitigate this, various dehazing techniques have been proposed, including Color Attenuation[10], non-local methods [11], end-to-end dehazing[12], Dark Channel Prior (DCP)[13], Adaptive dehazing method [14], [15].

For heterogeneous fog, additional techniques based on multiscale convolutional neural networks [16]and the use of both color and grayscale images [16], [17], have been developed. Single-image dehazing approaches, such as AOD-Net [18], GFN [19], GridDehazeNet [20], and MSCNN-HED [21], have also been explored. Furthermore, adversarial learning has been employed to generate more realistic dehazed images, as seen in methods like DCPDN [22], [23], DehazeGAN [24], and EPDN [25], which build on the Pix2Pix framework [26]. Light-Invariant Dehazing Networks (LIDN)[27], integrate components such as feature extractors, atmospheric light estimators, and encoder-decoder architectures to handle varying lighting conditions.

Dehazing not only improves image quality but also enhances vision-related applications by producing denoised images with higher clarity. In foggy images, low-intensity RGB pixels can be processed via fog transmission maps to generate clearer visuals. This process typically requires high-capacity training models, for which convolutional neural networks (CNNs) are well-suited due to their parameter efficiency and compatibility with GPU acceleration [3].

This paper proposes a refined autoencoder-based image-defogging technique, emphasizing enhanced feature extraction. Unlike traditional models that reconstruct full images, our method focuses on identifying and learning noise patterns, simplifying the noise regeneration and removal process. The effectiveness of the proposed model is evaluated using the RESIDE dataset, demonstrating notable improvements in fog removal and image clarity.

The paper is structured as follows: Section 2 presents a literature review; Section 3 describes the proposed technique and model architecture. Section 4 details the training procedure. Section 5 reports the results and discusses comparisons with existing methods. Finally, Section 6 concludes the study.

II. Literature Review

This section presents key research efforts addressing advancements in image defogging, particularly within the context of autonomous vehicle vision systems under foggy conditions. Given the safety-critical nature of object recognition in adverse weather, this domain has received considerable attention.

Chen et al. [28], proposed a Convolutional Autoencoder (CAE) for single-image defogging, leveraging densely connected networks for both encoding and decoding. Unlike traditional methods based on atmospheric scattering models, CAE was trained on paired clean and foggy images, outperforming eight state-of-the-art approaches while maintaining computational efficiency.

Paven et al. [29], introduced LCA-Net, a lightweight convolutional encoder-decoder network designed for image dehazing. By balancing network complexity and image quality, LCA-Net enables real-time dehazing without relying on atmospheric models, using convolutional layers for feature extraction and deconvolutional layers for image reconstruction.

Yifei Zhang [30], compared simple autoencoders (SAE) with convolutional autoencoders (CAE) in image processing, finding that CAE achieved superior denoising performance and lower MSE loss, producing sharper images. The study concluded that CAE offers distinct advantages over SAE in noise reduction tasks.

Despite their promise, traditional autoencoders exhibit limitations, such as difficulty controlling hidden-layer representations, overemphasis on relational structures, and loss of key data relationships. To overcome these Qinxue Meng et al. [31], proposed the Relational Autoencoder, designed to capture both feature-level and relational data characteristics. They further extended this architecture to variants including Variational, Sparse, and Denoising Autoencoders, demonstrating improved classification and robustness across common datasets.

Fazlali Hamidreza et al. [32], presented a deep convolutional autoencoder approach that separates the dehazing process into encoder and decoder stages. They

introduced artificial cloud-like data via a multi-scale super-pixel method. Compared to DCP, NLD, DehazeNet, and AOD-Net, their method produced higher quality outputs and avoided excessive image darkening, preserving detail in low-intensity regions.

Akshay Juneja et al. [33], developed Aethra-Net, a fog-removal algorithm for images and videos. It uses a vessel enhancement filter and an autoencoder to estimate transmission maps, then applies Airlight compensation. Aethra-Net achieves notable performance with low computational complexity, making it suitable for real-time, software-based applications.

To address limitations in deep learning dehazing models, K. Liu et al. [34], proposed a hybrid architecture combining DenseNet and Denoising Autoencoders (DAE). Their DAE-DenseNet model significantly improved image reconstruction quality, achieving a PSNR of 22.6, surpassing conventional methods while avoiding color oversaturation.

A.Ray et al.[35], Introduced an encoder-decoder model inspired by the Tiramisu architecture for deep learning-based dehazing. They evaluated its performance using the NTIRE 2018 Dehazing Challenge's SOTS dataset, reporting competitive results for both indoor and outdoor scenes.

While previous methods have made significant strides in fog and noise removal, the Noise Learning Denoising Autoencoder (NLDAE) model offers unique features that enhance its performance, particularly in real-time applications. Unlike traditional methods that rely on training models with clean images to restore noisy inputs, the NLDAE model is trained directly on the noise (fog) itself. This allows the model to learn the specific characteristics of fog and efficiently extract it from the noisy image. By subtracting the learned fog from the input, the model can recover a cleaner image with higher accuracy. This novel approach not only improves denoising performance but also makes the model highly adaptable for real-time usage, as it eliminates the need for additional clean image data, making it more efficient and suitable for dynamic, real-world scenarios.

Table 1 summarizes the reviewed fog and haze removal techniques. Traditional approaches such as DCP and color attenuation models offer simplicity and efficiency but struggle under dense fog and lack real-time capability. Deep learning models, including CNNs, autoencoders, and GANs, have significantly improved dehazing quality, yet often come with high computational costs. Recent advances leverage lightweight architectures (e.g., LCA-Net, AETHRA-Net) and vision transformers to achieve real-time performance while maintaining high visual quality. However, many methods still face challenges in generalizing varying fog densities, complex scenes, or low-light conditions, highlighting the ongoing need for efficient, robust, and scalable solutions.

Table 1: Comparative Summary of Related Dehazing and Denoising Methods

Year	Ref. No.	Model	Advantages	Limitations
2015	Q. Zhu et al. [10]	Color Attenuation	Enhances dehazing using color and contrast separation	Less effective in dense fog
2016	Berman et al. [11]	Non-local Method	Utilizes non-local information	Computationally intensive
2018	Cai et al. [12]	Deep Learning End-to-End Dehazing	Fully automatic dehazing using neural networks	Requires large datasets
2009	He et al. [13]	DCP	Popular and interpretable approach	May produce halo artifacts
2017	Li et al.[15]	Adaptive Dehazing	Adapts to variable fog densities	Complex to implement
2016	Ren et al. [16]	Multi-scale CNN	Handles heterogeneous fog well	Deep network needed
2010	Tarel et al.[18]	Color& Grayscale Input	Uses multiple image types for better accuracy	Increased complexity
2017	Wang et al.[18]	AOD-Net	Direct end-to-end fog removal	Limited under variable lighting
2018	Zangh et al.[19]	GFN	Guided dehazing with good quality	Needs large training sets
2020	Chen et al. [20]	GridDehazeNet	Grid-based processing improves accuracy	Complex structure
2020	Pan et al[21]	MSCNN-HED	Better structural detail preservation	Resource-intensive
2019	Goodfellow et al.[22]	DCPDN	Combines classic and adversarial learning	Complicated training
2018	Zhu et al.[24]	GAN	Generates realistic outputs	Needs careful tuning
2019	Qu et al.[25]	EPDN	Handles lighting variation	Sensitive to training quality
2021	Ghosh et al.[27]	LIDN	Deals with lighting issues effectively	High complexity
2020	Chen et al. [28]	Dense Convolutional Autoencoder	Outperformed 8 SOTA methods while maintaining efficiency	Requires paired fog/clean images
2021	Paven et al. [29]	Lightweight CNN Autoencoder	Real-time dehazing without atmospheric model	May trade off some quality
2019	Yifei Zhang [30]	CAE vs SAE Comparison	CAE achieved lower MSE, sharper images	SAE had weaker denoising
2022	Qinxue Meng [31]	Advanced Autoencoder Variants	Better representation learning with improved robustness	Complexity in architecture
2021	Fazlali Hamidreza [32]	Deep Convolutional AE	High output quality; preserved details vs DCP, NLD, AOD-Net	Introduced synthetic data complexity
2022	Akshay Juneja [33]	AE + Vessel Filter	Suitable for videos; low computational cost	May have domain-specific limitations
2022	K. Liu [34]	DAE + DenseNet Hybrid	High PSNR (22.6), better reconstruction, no oversaturation	Increased model complexity
2019	A. Ray [35][35]	Encoder-Decoder (Tiramisu-based)	Strong results on NTIRE 2018 dataset	Generalization to real-world scenes not discussed

III. Methodology

In this study, we employ the Noise Learning-based Denoising Autoencoder (NLDAE) framework [36], to tackle the complex task of image restoration in foggy conditions. This work utilizes the NLDAE framework, which builds upon and modifies the traditional Denoising Autoencoder (DAE) [37], architecture. We focus on *enhancing its feature extraction capabilities*. Notable improvements include architectural optimizations, the integration of skip connections, and effective data augmentation techniques. The accuracy and effectiveness of the restoration process eventually increased as a result of these improvements, which enabled the framework to capture the crucial characteristics required for dehazing more accurately.

The NLDAE concentrates on learning the noise characteristics (haze) from the input data, in contrast to the

traditional DAE[38], which maps noisy images to clean ones directly. By deducting the predicted noise from the hazy observation, the trained model eliminates the haze and restores the clear image. This method makes use of the presumption that the haze has simpler statistical characteristics than the original image, allowing for more accurate and efficient restoration.

A. Traditional Denoising Autoencoder

Feature extraction, dimensionality reduction, and unsupervised learning are the main applications of the conventional Autoencoder (AE) [38], a deep learning model. The AE is made up of two primary parts when it comes to image denoising:

- Encoder: A series of convolutional layers (kernel size = 3×3 , stride = 1) with ReLU activation, followed by max-pooling (2×2) to downsample

spatial dimensions. Batch normalization is applied after each convolution, while removing less important information, including noise, the encoder preserves the image's most important properties [39].

- **Latent Space:** The bottleneck layer compresses the input into a 256-dimensional vector.
- **Decoder:** Transposed convolution (kernel size = 3×3 , stride = 1) with ReLU activation, followed by upsampling, aims to produce an output image that nearly resembles the original clean image.

The DAE[37] is trained to minimize the Mean Squared Error (MSE) loss between the associated clean image and the noisy input image in denoising tasks.

- **Loss Function:** Mean Squared Error (MSE) between the clean ground truth and the reconstructed image.

As shown in Figure 1, the encoder and decoder work in harmony to effectively remove noise and reconstruct a clean image, where X represents the blurred image and Y represents the image after dehazing. However, non-random noise with defined patterns and dependencies, such as haze, is difficult for typical DAEs to handle. The NLDAE was created to address this constraint.

- **Optimizer:** Adam (learning rate = 0.001, $\beta_1 = 0.9$, $\beta_2 = 0.999$).
- **Limitation:** Struggles with structured noise (e.g., haze) due to direct image reconstruction.

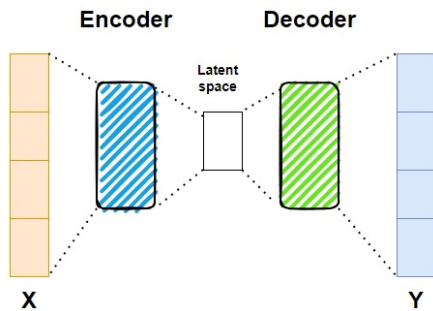


Figure 1: Traditional Denoising Autoencoder

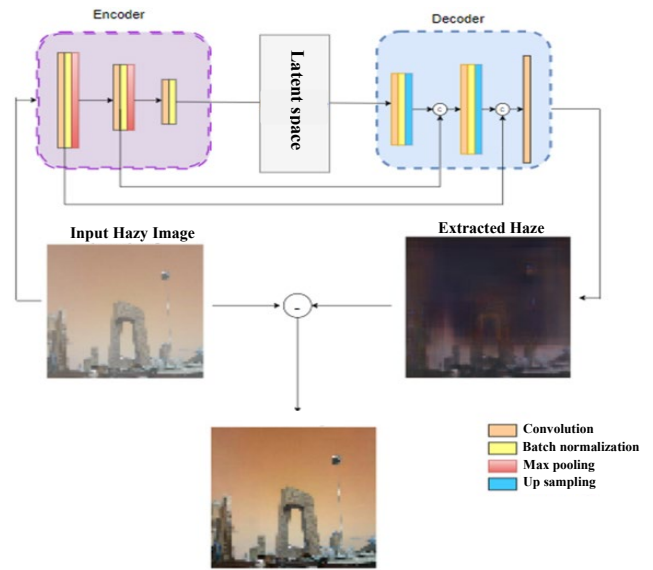


Figure 2: Proposed Model Architecture Diagram

B. Proposed Method

NLDAE [36] introduces an innovative approach to dehazing. Instead of reconstructing the entire clean image, as in traditional DAEs, NLDAE is specifically trained to learn and regenerate the haze (noise) from foggy input images. The haze is then subtracted from the noisy image to produce a clean version. As illustrated in Figure 2, the architecture implements a systematic haze removal process through four key components:

- **Encoder:** (five convolutional blocks with max-pooling) progressively extracts and downsamples multi-scale features while separating haze patterns from clean components.
- **Bottleneck (Latent Space):** The latent space provides a compressed representation of the image, embedding crucial spatial and structural patterns[40], including haze characteristics. This stage facilitates learning the unique statistical properties of the haze.
- **Decoder:** The decoder reconstructs the haze component from the latent space using transposed convolutional layers (five transposed convolutional blocks) for upsampling. Skip connections retain spatial details lost during downsampling, ensuring accurate haze reconstruction.
- **Haze Subtraction Module:** Generates the final clean image ($\hat{I} = I_{\text{input}} - \hat{h}$). The model is trained using a composite loss function ($\text{MSE} + \lambda \cdot \text{SSIM}$, $\lambda=0.1$) with AdamW optimization (initial LR= $1e-4$, cosine decay), achieving superior dehazing through targeted noise estimation while maintaining computational efficiency for real-time applications.

In this case, the target output is the haze component, and the network is optimized to predict haze from the noisy input. The final clean image is obtained by subtracting the predicted haze from the blurry image, providing a practical and effective solution for image dehazing.

C. Dataset

In this study, the suggested NLDAE for fog removal in autonomous vehicle applications was trained and evaluated using the RESIDE [41], dataset [42], which offers a comprehensive collection of foggy images captured in both indoor and outdoor settings. This dataset enables the evaluation of dehazing algorithms under diverse conditions. To further assess the model's generalization ability in real-world scenarios, additional experiments were conducted on the Foggy Cityscapes dataset[43], which contains synthetic fog applied to real-world urban driving scenes. This evaluation highlights the model's robustness across different domains and fog densities.

1) Data

Both interior and outdoor photos taken in different foggy circumstances are included in the RESIDE [41], Two subgroups were used for this study. With 13,900 photos captured in various indoor situations with different fog levels, lighting, and interior configurations. The outside dataset comprises 62,212 photos that show outdoor sceneries under foggy circumstances, including rural landscapes, highways, and urban streets.

Furthermore, two test sets were used to assess the trained model's performance. SOTS (Synthetic and Outdoor Test Set), 500 photos from the RESIDE dataset, is used to evaluate how well the model generalizes to synthetic and outdoor foggy photographs. Particularly pertinent to autonomous driving applications is the HSTS (Highway and Street Test Set), a smaller collection of 20 photos that concentrates on outside landscapes taken in highway and street settings.

2) Data Characteristics

A wide range of photos representing different fog densities and conditions is included in the dataset. The model can comprehend how fog acts in constrained areas with varying sight and lighting levels. The outdoor photos, on the other hand, show intricate real-world situations with a variety of fog intensities, lighting conditions, and scene compositions, such as urban traffic, highways, and rural places.

3) Data Preprocessing

We implemented a rigorous preprocessing pipeline involving: Firstly, pixel normalization to the [0,1] range. Secondly, comprehensive data augmentation including geometric transformations ($\pm 15^\circ$ rotation, horizontal flipping) and photometric adjustments ($\pm 20\%$ brightness/contrast variations), and finally, strategic dataset

partitioning (80% training, 10% validation, 10% testing) with fog-density stratification (mild/moderate/heavy). The SOTS (500 images) and HSTS (20 images) subsets were reserved exclusively for benchmarking, while Foggy Cityscapes data was incorporated to enhance domain generalization. All preprocessing operations were implemented using TensorFlow's data pipeline with deterministic seeding to ensure reproducibility across experiments.

IV. Model Training

The training procedure, optimization parameters, and evaluation approach for the suggested Noise Learning-based Denoising Autoencoder are described in this part.

A. Training Setup

The foggy photos from the RESIDE dataset were used to train the NLDAE model, and the setup for the training procedure was as follows. The pixel-by-pixel difference between the ground truth haze and the expected haze was computed using the Mean Squared Error (MSE) loss function. To reduce overfitting, the Adam optimizer was used with weight decay, momentum parameters ($\beta_1 = 0.9$, $\beta_2 = 0.999$), and an initial learning rate of 0.0001. In order to balance model convergence and computing performance, a batch size of 16 was used. Early stopping was used to check validation loss and avoid overfitting during the 50 epochs of training.

B. Data Augmentation

Data augmentation methods were used during training to improve the model's generalization and resilience. These included resizing photographs by random scale factors to replicate varied object sizes, rotating the images randomly within a range of ± 15 degrees to simulate different views, flipping the images horizontally to introduce variances, and varying brightness levels to simulate different lighting situations.

C. Energy and Efficiency Optimization

To address the energy consumption of training deep neural networks, several efficiency strategies were adopted. The model was trained using Mixed Precision Training, which enables faster computation and reduced GPU memory usage by combining 16-bit and 32-bit floating-point operations. Additionally, Early stopping was utilized to prevent unnecessary training epochs, and the batch size was tuned to optimize GPU utilization while keeping memory demand low. These measures collectively contributed to reducing both training time and energy consumption.

D. Hardware and Framework

The model was implemented using Tensor Flow and Keras libraries and trained on an NVIDIA GPU (RTX 4060) with 16 GB RAM, core i7 enabling efficient processing of high-resolution images. The training process

was conducted over several hours, depending on the dataset size and hardware capabilities.

E. Evaluation Strategy

After training, the model's performance was evaluated using two distinct test datasets: SOTS and HSTS. Key evaluation metrics included Peak Signal-to-Noise Ratio (PSNR) and Structural Similarity Index (SSIM). A higher PSNR value indicates better image restoration quality by measuring the fidelity between the original and dehazed images. Meanwhile, SSIM assesses the perceptual similarity between the restored and ground truth images, reflecting how closely the dehazed output resembles the original image from a human visual perspective.

V. Results and discussions

The results of the Noise Learning-based Denoising Autoencoder (NLDAE) on the RESIDE dataset are shown and examined in this section.

A. Performance on Indoor Dataset

Using the Indoor SOTS and HSTS subsets, the indoor testing was conducted with different fog densities. The model performed better than outdoor data on the SOTS test set, with a PSNR of 29.87 and an SSIM of 0.966. This is because indoor fog patterns are simpler and more predictable. The NLDAE obtained a PSNR of 25.61 and an SSIM of 0.945 on the HSTS test set in high-density indoor fog conditions. These measurements validate the model's capacity to successfully minimize haze and preserve important information in more difficult settings, even though they are marginally lower than the SOTS findings.

B. Performance on Outdoor Dataset

With a PSNR of 25.14 and an SSIM of 0.930 on the SOTS test set, the NLDAE effectively removed haze while maintaining structural details. The model's ability to preserve important visual characteristics necessary for tasks like object detection in autonomous cars is demonstrated by its strong SSIM score. The model's performance on the HSTS test set, which concentrates on high-density fog scenarios, was somewhat better than that of the conventional outdoor test set, with a PSNR of 26.03 and an SSIM of 0.939, demonstrating its resilience in handling difficult conditions.

C. Discussion

The outcomes demonstrate how well the NL DAE model performs dehazing tasks in a variety of scenarios. Because indoor illumination and haze patterns are more consistent and predictable than outside ones, the model performed better on indoor photos in terms of PSNR and SSIM.

On the other hand, because of their dynamic haze patterns, varied lighting, and intricate textures, outdoor photos posed further difficulties. With only a minor decline

in performance when compared to the SOTS subsets, the NLDAE proved resilient in high-density fog scenarios (HSTS), demonstrating its versatility and capacity to successfully restore visibility under trying circumstances.

The NLDAE model takes a novel approach in contrast to conventional methods by learning to remove haze instead of directly reconstructing the clear image. By reducing the statistical complexity of haze removal, this strategy helps the model avoid the overfitting and overcomplication problems that are common in traditional approaches, while still achieving better image clarity and increased computational efficiency.

The strong performance on both indoor and outdoor datasets highlights its potential for real-world uses, especially in autonomous car systems where improved visibility is essential for tasks like object detection and bad weather navigation.

Table 2: QUANTITATIVE COMPARISON OF TRADITIONAL DEHAZING METHODS ON HSTS AND SOTS OUTDOOR DATASETS.

Method	PSNR		SSIM	
	HSTS	SOTS	HSTS	SOTS
DehazeNet [12]	24.49	22.46	0.915	0.851
MSCNN[21]	18.29	19.56	0.841	0.863
AOD-Net[18]	21.58	20.29	0.922	0.876
GFN [19]	22.49	21.55	0.874	0.844
Proposed Work (NLDAE)	26.03	25.14	0.939	0.930

Table 3: QUANTITATIVE COMPARISON OF TRADITIONAL DEHAZING METHODS ON HSTS AND SOTS INDOOR DATASETS.

Method	PSNR		SSIM	
	HSTS	SOTS	HSTS	SOTS
DehazeNet[12]	--	21.14	--	0.847
MSCNN[21]	--	17.57	--	0.810
AOD-Ne[18]	--	19.06	--	0.814
GFN [19]	--	22.30	--	0.856
Proposed Work (NLDAE)	25.61	29.87	0.945	0.966

Table 2 shows the results of our quantitative evaluation of many dehazing techniques using the HSTS and SOTS datasets' PSNR and SSIM values. The NLDE model outperformed deep learning-based techniques (like AOD-Net[18] and GFN [21]) as well as more conventional techniques (like DehazeNet [12]) in terms of picture restoration quality. It obtained the highest PSNR and SSIM scores, which are indicated in red. This outcome shows how well NLDE works to improve visual quality and clarity.

Table 3 presents a detailed comparison of various dehazing methods, including DehazeNet[44], MSCNN[21], AOD-Net[18], GFN[19], and the proposed NLDE model, evaluated on the HSTS and SOTS indoor datasets. Notably, the methods DehazeNet, MSCNN, AOD-Net, and GFN did not report results for the HSTS dataset. On the other hand, the NLDE model outperforms all other methods on both datasets, achieving the highest PSNR and SSIM values, with 25.61 (PSNR) and 0.945 (SSIM) on HSTS, and 29.87 (PSNR) and 0.966 (SSIM) on SOTS. These results demonstrate the superior dehazing performance of NLDE.

In comparing the proposed model with autoencoder-based dehazing approaches such as the Tiramisu Auto-Encoder [35], UCL-Dehaze [45], IC-Dehazing [46], Convolutional AutoEncoder [28], LCA-Net[29], deep convolutional autoencoder [32], Aethra-net[33], DehazeNet [47],[48], and DenseNet [34], notable performance distinctions emerge.

Table 4 presents a quantitative comparison of various dehazing methods based on their PSNR and SSIM scores on RESIDE datasets. The NIDE model demonstrates the highest performance with a PSNR of 29.87 and an SSIM of 0.966, significantly outperforming both earlier and recent methods. Among recent approaches, Tiramisu Auto-Encoder (2024) and VNet (2024) [48] also achieve strong results, with PSNR values of 29 and 28.5, respectively. However, models like Aethra-net and UCL-Dehaze show notably lower performance, highlighting the effectiveness of advanced architectures like NIDE for dehazing tasks.

In some studies, higher PSNR and SSIM values have been achieved; however, these improvements often come at the cost of significantly increased model complexity. This added complexity results in substantially longer processing times, making such approaches less suitable for real-time applications where speed is a critical factor. For instance, Y.cui et al.[49], and Y.wang et al.[50]. Demonstrate notable enhancements in image quality metrics but rely on deep architectures with extensive computations, leading to impractical latency for real-world deployment. Our model, by contrast, strikes an effective balance between high performance and computational efficiency, making it well-suited for real-time systems. Therefore, while accuracy is essential, maintaining this balance is critical for practical applications.

These examples highlight the inherent trade-off between model complexity and computational efficiency. Prioritizing techniques that balance speed and quality is crucial in real-world applications, particularly those that call for real-time processing, like surveillance, autonomous cars, or medical imaging. Despite having better measurements, overly complicated models could not be able to provide the responsiveness required in these situations, which would ultimately restrict their usefulness.

Table 4: QUANTITATIVE COMPARISON OF DEHAZING METHODS BASED ON AUTOENCODER ON RESIDE DATASETS.

Method	PSNR	SSIM
CAE(2019) [28]	24.56	0.9126
LCA-Net(2020) [29]	24.734	0.8951
DCAE(2020) [33]	24.63	0.93
Aethra-net(2023) [33]	16.408	0.7
IC-Dehazing(2023) [46]	22.56	0.894
UCL-Dehaze(2024) [45]	21.36	0.862
DenseNet(2024) [34]	22.60	0.8633
VNet (2024) [48]	28.5	0.92
Tiramisu Auto-Encoder(2024) [35]	29	0.94
Proposed Work (NLDAE)	29.87	0.966

Table 5: PERFORMANCE ON FOGGY CITYSCAPES DATASET UNDER DIFFERENT TRAINING SETTINGS AND FOG DENSITIES.

Training data type	Fog Density	PSNR	SSIM
Indoor	Moderate	27.05	0.934
Indoor	Dense	25.03	0.925
Outdoor	Moderate	24.07	0.897
Outdoor	Dense	21.06	0.880

D. Real-World Foggy Cityscapes Dataset

To evaluate the generalization capability of the proposed model under real-world scenarios, we conducted experiments on the Foggy Cityscapes dataset, which features urban outdoor scenes with synthetic fog that closely mimics natural fog. The assessment was performed using two training settings: in the first, the model was trained on indoor hazy images and tested on Foggy Cityscapes; in the second, it was trained on outdoor hazy images and similarly tested on the same dataset. Furthermore, to examine the model's robustness under different fog conditions, we tested subsets of the dataset categorized by fog density (moderate and dense). The results, summarized in Table 5, indicate that the proposed approach maintains competitive performance across various fog levels, demonstrating strong generalization in challenging real-world environments.

E. Computational Performance Evaluation

To assess the real-time feasibility of NLDAE, latency and GPU memory metrics were measured. The model achieved an average latency of 107.35 ms per image, with a peak of 292.42 ms and a minimum of 62.84 ms. GPU memory consumption remained within 6585 MB out of the available 8188 MB, indicating that the model is well-suited for

deployment in real-time or near real-time autonomous driving systems.

F. Limitations and Future Work

While even Although the NLDAE model produced encouraging results, there are still some drawbacks. Using multi-scale feature extraction techniques or adding more contextual information could enhance its effectiveness in exceedingly complicated outdoor scenes. Furthermore, the model's performance in other weather scenarios, such as rain or snow, has not yet been assessed, underscoring the need for more research.

VI. Conclusion

In order to tackle the difficulties of dehazing, especially for autonomous cars operating in bad weather circumstances like fog, we applied the Noise Learning-based Denoising Autoencoder (NLDAE) in this study. The NLDAE specifically concentrates on learning haze (noise) patterns and efficiently eliminating them to improve image visibility, in contrast to conventional denoising autoencoders.

We implemented several feature extraction improvements to further boost the framework's efficiency, such as architectural optimizations, the incorporation of skip connections to maintain multi-level details, and sophisticated data augmentation methods to increase the training dataset.

The RESIDE dataset, encompassing both indoor and outdoor scenes with dense fog, was used to train and evaluate the framework. The model achieved strong performance on the SOTS and HSTS test sets, with PSNR up to 29.87 and SSIM up to 0.966. It also showed robustness in dense fog and performed better on indoor scenes, reflecting the impact of scene complexity. Evaluation on the Foggy Cityscapes dataset confirmed the model's generalization, achieving PSNR/SSIM of 27.05/0.934 in moderate fog and maintaining competitive results in dense fog across various training scenarios.

REFERENCE

- [1] K. Muhammad, A. Ullah, J. Lloret, J. D. Ser, and V. H. C. de Albuquerque, "Deep Learning for Safe Autonomous Driving: Current Challenges and Future Directions," *IEEE Transactions on Intelligent Transportation Systems*, vol. 22, no. 7, pp. 4316-4336, 2021, doi: 10.1109/tits.2020.3032227.
- [2] Mohammed and Rahimoddin, "Artificial Intelligence-Driven Robotics for Autonomous Vehicle Navigation and Safety," *NEXG AI Review of America*, 2022.
- [3] Y. Wiseman, "Autonomous vehicles," in *Research anthology on cross-disciplinary designs and applications of automation*, 2022.
- [4] I. Ogunrinde and S. Bernadin, "A Review of the Impacts of Defogging on Deep Learning-Based Object Detectors in Self-Driving Cars," presented at the SoutheastCon 2021, 2021.
- [5] X. Zhao, T. Zhang, W. Chen, and W. Wu, "Image Dehazing Based on Haze Degree Classification," presented at the 2020 Chinese Automation Congress (CAC), 2020.
- [6] E. Yurtsever, J. Lambert, A. Carballo, and K. Takeda, "A survey of autonomous driving: Common practices and emerging technologies," *IEEE access*, vol. 8, pp. 58443-58469, 2020.
- [7] Y. Zhang, A. Carballo, H. Yang, and K. Takeda, "Perception and sensing for autonomous vehicles under adverse weather conditions: A survey," *ISPRS Journal of Photogrammetry and Remote Sensing*, vol. 196, pp. 146-177, 2023, doi: 10.1016/j.isprsjprs.2022.12.021.
- [8] G. Bathla et al., "Autonomous Vehicles and Intelligent Automation: Applications, Challenges, and Opportunities," *Mobile Information Systems*, vol. 2022, pp. 1-36, 2022, doi: 10.1155/2022/7632892.
- [9] Z. H. Arif et al., "Comprehensive Review of Machine Learning (ML) in Image Defogging: Taxonomy of Concepts, Scenes, Feature Extraction, and Classification techniques," *IET Image Processing*, vol. 16, no. 2, pp. 289-310, 2021, doi: 10.1049/ipr2.12365.
- [10] Q. Zhu, J. Mai, and L. Shao, "A Fast Single Image Haze Removal Algorithm Using Color Attenuation Prior," *IEEE Trans Image Process*, vol. 24, no. 11, pp. 3522-33, Nov 2015, doi: 10.1109/TIP.2015.2446191.
- [11] D. Berman, T. Treibitz, and S. Avidan, "Non-Local Image Dehazing," in *Proceedings of the IEEE conference on computer vision and pattern recognition*, 2016.
- [12] B. Cai, X. Xu, K. Jia, C. Qing, and D. Tao, "Dehazenet: An end-to-end system for single image haze removal," *IEEE transactions on image processing*, vol. 25, no. 11, pp. 5187-5198, 2016.
- [13] K. He, J. Sun, and X. Tang, "Single image haze removal using dark channel prior," *IEEE transactions on pattern analysis and machine intelligence*, 2010.
- [14] I. Yoon, S. Jeong, J. Jeong, D. Seo, and J. Paik, "Wavelength-adaptive dehazing using histogram merging-based classification for UAV images," *Sensors (Basel)*, vol. 15, no. 3, pp. 6633-51, Mar 19 2015, doi: 10.3390/s150306633.
- [15] Y. Li, N. Wang, J. Liu, and X. Hou, "Demystifying Neural Style Transfer," *arXiv preprint arXiv:1701.01036*, 2017.

- [16] J.-P. Tarel and N. Hautiere, "Fast visibility restoration from a single color or gray level image," presented at the 2009 IEEE 12th International Conference on Computer Vision, 2009.
- [17] J.-P. Tarel, N. Hautiere, A. Cord, D. Gruyer, and H. Halmaoui, "Improved Visibility of Road Scene Images under Heterogeneous Fog," in *2010 IEEE intelligent vehicles symposium*, 2010.
- [18] B. Li, X. Peng, Z. Wang, J. Xu, and D. Feng, "AOD-Net: All-in-One Dehazing Network," in *Proceedings of the IEEE international conference on computer vision*, 2017.
- [19] W. a. M. Ren, Lin and Zhang, Jiawei and Pan, Jinshan and Cao, Xiaochun and Liu, Wei and Yang, Ming-Hsuan, "Gated fusion network for single image dehazing," in *Proceedings of the IEEE conference on computer vision and pattern recognition*, vol. 48, no. 5), 2018, pp. vii-ix.
- [20] X. Liu, Y. Ma, Z. Shi, and J. Chen, "GridDehazeNet: Attention-Based Multi-Scale Network for Image Dehazing," in *Proceedings of the IEEE/CVF international conference on computer vision*, 2019.
- [21] W. Ren, J. Pan, H. Zhang, X. Cao, and M.-H. Yang, "Single Image Dehazing via Multi-scale Convolutional Neural Networks with Holistic Edges," *International Journal of Computer Vision*, vol. 128, no. 1, pp. 240-259, 2019, doi: 10.1007/s11263-019-01235-8.
- [22] I. Goodfellow et al., "Generative Adversarial Nets," *Advances in neural information processing systems*, 2014.
- [23] H. Zhang and V. M. Patel, "Densely connected pyramid dehazing network," in *Proceedings of the IEEE conference on computer vision and pattern recognition*, 2018, pp. 3194-3203.
- [24] H. Zhu, X. Peng, V. Chandrasekhar, L. Li, and J.-H. Lim, "DehazeGAN: When Image Dehazing Meets Differential Programming," 2018.
- [25] Y. Qu, Y. Chen, J. Huang, and Y. Xie, "Enhanced Pix2pix Dehazing Network," in *Proceedings of the IEEE/CVF conference on computer vision and pattern recognition*, 2019.
- [26] Y. Qu, Y. Chen, J. Huang, and Y. Xie, "Enhanced pix2pix dehazing network," in *Proceedings of the IEEE/CVF conference on computer vision and pattern recognition*, 2019, pp. 8160-8168.
- [27] A. Ali, A. Ghosh, and S. S. Chaudhuri, "LIDN: a novel light invariant image dehazing network," *Engineering Applications of Artificial Intelligence*, 2023.
- [28] R. Chen and E. M.-K. Lai, "CONVOLUTIONAL AUTOENCODER FOR SINGLE IMAGE DEHAZING," in *ICIP*, 2019.
- [29] A. Bennur, M. Gagggar, and other, "LCA-Net: Light Convolutional Autoencoder for Image Dehazing," *arXiv preprint arXiv:2008.10325*, 2020.
- [30] Y. Zhang, "A better autoencoder for image: Convolutional autoencoder," in *ICONIP17-DCEC*. Available online: http://users.cecs.anu.edu.au/Tom.Gedeon/conf/ABCs2018/paper/ABCs2018_paper_58.pdf (accessed on 23 March 2017), 2018.
- [31] Q. Meng, D. Catchpole, D. Skillicom, and P. J. Kennedy, "Relational Autoencoder for Feature Extraction," in *2017 International joint conference on neural networks (IJCNN)*, 2017.
- [32] H. Fazlali, S. Shirani, M. McDonald, D. Brown, and T. Kirubarajan, "Aerial image dehazing using a deep convolutional autoencoder," *Multimedia Tools and Applications*, vol. 79, no. 39-40, pp. 29493-29511, 2020, doi: 10.1007/s11042-020-09383-7.
- [33] A. Juneja, V. Kumar, and S. K. Singla, "Aethra-net: Single image and video dehazing using autoencoder," *Journal of Visual Communication and Image Representation*, vol. 94, 2023, doi: 10.1016/j.jvcir.2023.103855.
- [34] K. Liu, Y. Yang, Y. Tian, and H. Mao, "Image Dehazing Technique Based on DenseNet and the Denoising Self-Encoder," *Processes*, vol. 12, no. 11, 2024, doi: 10.3390/pr12112568.
- [35] A. Ray and S. Sharanya, "Single Image Dehazing Using A Tiramisu Auto-Encoder," in *2024 International Conference on Intelligent Systems for Cybersecurity (ISCS)*, 2024.
- [36] W.-H. Lee, M. Ozger, U. Challita, and K. W. Sung, "Noise Learning-Based Denoising Autoencoder," *IEEE Communications Letters*, vol. 25, no. 9, pp. 2983-2987, 2021, doi: 10.1109/lcomm.2021.3091800.
- [37] D. Bank, N. Koenigstein, and R. Giryes, "Autoencoders," *Machine learning for data science handbook: data mining and knowledge discovery handbook*, 2023.
- [38] R. Singh, A. K. Dubey, and R. Kapoor, "Denoised Autoencoder using DCNN Transfer Learning Approach," presented at the 2022 International Mobile and Embedded Technology Conference (MECON), 2022.
- [39] W. K. Mutlag, S. K. Ali, Z. M. Aydam, and B. H.Taher, "Feature Extraction Methods: A Review," *Journal of Physics: Conference Series*, 2020.
- [40] Chen et al., "Multi-feature based Foggy Image Classification," *IOP Publishing*, 2019.
- [41] B. Li et al., "Benchmarking Single Image Dehazing and Beyond," *IEEE Trans Image Process*, Aug 30 2018, doi: 10.1109/TIP.2018.2867951.
- [42] A. Juneja, V. Kumar, and S. K. Singla, "A Systematic Review on Foggy Datasets:

- Applications and Challenges," *Archives of Computational Methods in Engineering*, vol. 29, no. 3, pp. 1727-1752, 2021, doi: 10.1007/s11831-021-09637-z.
- [43] M. Cordts *et al.*, "The cityscapes dataset," in *CVPR Workshop on the Future of Datasets in Vision*, 2015, vol. 2, p. 1.
- [44] R. Sassi *et al.*, "PDF-ECG in clinical practice: A model for long-term preservation of digital 12-lead ECG data," *J Electrocardiol*, vol. 50, no. 6, pp. 776-780, Nov-Dec 2017, doi: 10.1016/j.jelectrocard.2017.08.001.
- [45] Wang *et al.*, "Ucl-dehaze: Towards real-world image dehazing via unsupervised contrastive learning," *IEEE Transactions on Image Processing*, 2024.
- [46] F. Twisk, "Rebuttal to Ickmans et al. association between cognitive performance, physical fitness, and physical activity level in women with chronic fatigue syndrome. J Rehabil Res Dev. 2013;50(6):795-810.
www.rehab.research.va.gov/jour/2013/506/pdf/ickmans506.pdf," *J Rehabil Res Dev*, vol. 50, no. 9, pp. vii-viii, 2013. [Online]. Available:
<https://www.ncbi.nlm.nih.gov/pubmed/24458970>.
- [47] W. Li, D. Fan, Q. Zhu, Z. Gao, and H. Sun, "HEDehazeNet: Unpaired image dehazing via enhanced haze generation," *Image and Vision Computing*, vol. 150, 2024, doi: 10.1016/j.imavis.2024.105236.
- [48] Q. Sun, Z. Yang, R. Li, and Y. You, "VDNet: An Image Dehazing Model Based on the Variational Autoencoder," in *2024 36th Chinese Control and Decision Conference (CCDC)*, 2024.
- [49] Y. Cui, W. Ren, and A. Knoll, *Omni-Kernel Network for Image Restoration*. 2024.
- [50] Y. Wang and B. He, "CasDyF-Net: Image Dehazing via Cascaded Dynamic Filters," *arXiv preprint arXiv:2409.08510*, 2024.